

Physical properties of predicted MAX phase borides Hf_2AB (A = Pb, Bi): a DFT insight

M. S. Hossain, M. A. Ali*, M. M. Hossain, and M. M. Uddin

Department of Physics, Chittagong University of Engineering and Technology (CUET), Chattogram-4349, Bangladesh

ABSTRACT

We have used density functional theory to study the recently predicted MAX phase borides Hf_2AB (A = Pb, Bi) in where the mechanical, electronic, thermal, and optical properties have been investigated for the first time. A good agreement of the obtained lattice constants with the reported values confirmed the well accuracy of the present calculations. The stiffness constants (C_{ij}) attest the mechanical stability of all title compounds. The mechanical behaviors have been scrutinized discreetly by considering the bulk modulus, shear modulus, Young's modulus, as well as hardness parameters. The brittle nature of Hf_2AB (A = Pb, Bi) borides has also been confirmed. The electronic band structure and density of states (DOS) revealed the metallic behavior of the titled materials. The anisotropy in electrical conductivity has been disclosed by considering the energy dispersion along different directions. The variation of Vickers hardness is explained in terms of total DOS of Hf_2AB (A = Pb, Bi). The anisotropic nature of mechanical properties of the phases has also been studied. The technologically important parameters (Debye temperature, minimum thermal conductivity, and Grüneisen parameter) have also been used to evaluate the thermal behaviors of the titled materials. The possibility of Hf_2AB (A = Pb, Bi) for use as coating materials has been assessed by studying the reflectivity.

Keywords: DFT study; MAX phase boride; mechanical properties; electronic properties; thermal properties; reflectivity.

1. Introduction

The prospective demand for the chemical diversity of MAX phases is growing in time due to their increasing applications in many sectors. The list of applications is also being longer because of the beneficial properties of metals and ceramics [1–4]. A large number of articles have been published regularly by reporting either their new member or opening the new door for possible applications. The driving force that encouraged scientists is the bridging of their properties such

*Corresponding author: ashrafphy31@cuet.ac.bd

as their conductivity (both electrical and thermal), machinability, and mechanical strength like metallic materials. On the other hand, their mechanical properties are good at high-temperature, their resistance to oxidation and corrosion is also high enough like ceramic materials [2,5–9]. The unique bridging of the aforementioned properties makes MAX phases one of the vital classes of materials and the research interest in these materials has been reflected from the exponential increase of the published articles [10]. To date, the number of known MAX phases crossed 150 mile-stone [11].

One of the limitations of MAX phases is that their diversity regarding X elements is confined within C and N for a long period as compounds [12–21] or solid solutions [22–31]. Thus, the extension of X elements beyond C/N can open the platform for a huge number of MAX phase members. The researchers have already found room for this extension by extending the X element to B (termed as MAX phase borides) owing to the bright prospect of B and its compounds [32]. It is now proven that the MAX phase borides are found as potential materials in many attractive fields [33–35]. Few numbers of MAX phase borides have also been successfully synthesized that make sure the possible extension of MAX phases in terms of borides. Racklet *et al.*[36,37] have synthesized the M_2SB (Zr, Hf and Nb) MAX phase borides, they were further investigated by Ali *et al.*[38] using first principles calculations. Another important MAX phase borides (212 MAX phase: Ti_2InB_2) has been synthesized by Wang *et al.* [39] and they were further investigated by Ali *et al.*[40] and Wang *et al.*[41]. Moreover, a number of MAX phase borides have also been predicted by the researchers. Khazaei *et al.*[42] have predicted the MAX phase borides for the first time and reported the formation energies, electronic and mechanical properties of M_2AIB ($M = Sc, Ti, Cr, Zr, Nb, Mo, Hf, \text{ or } Ta$) MAX phase borides. Later on, the Ti_2SiB [43], M_2AB ($M = Ti, Zr, Hf; A = Al, Ga, In$) [44], V_2AIB [10], and M_2AIB ($M = V, Nb, Ta$) [45] have been predicted theoretically and investigated their physical properties as well.

The last inclusion in this MAX phase group (MAX phase borides) is being reported by Miao *et al.*[46]. Recently, Miao *et al.*[46] have been predicted Hf_2AB ($A = Pb, Bi$) borides by confirming their thermo-dynamical stability. They have also studied the electronic properties including band structure, the density of states and electron localization function. As we know that the MAX phase materials have been found themselves in many sectors for practical applications and this limited information is not enough to predict whether these borides have also the potential for

applications in the fields where the MAX phase carbides or nitrides are already been used. To check this possibility, the physical properties of Hf_2AB ($A = \text{Pb, Bi}$) borides should be compared with their corresponding carbides and/or nitrides. It is also an attractive topic that whether the borides MAX phase can be the replacement of corresponding carbides and/or nitrides.

Therefore, in our current project, we have investigated the mechanical, electronic, thermal and optical properties along with theoretical Vickers hardness and mechanical anisotropy of Hf_2AB ($A = \text{Pb, Bi}$) borides for the first time. Moreover, the obtained physical properties of Hf_2AB ($A = \text{Pb, Bi}$) are compared with those of other Hf-based borides Hf_2AB ($A = \text{Al, Ga, In, S}$), where available.

2. Computational methodology

The physical properties of Hf_2AB ($A = \text{Pb, Bi}$) borides are computed via plane-wave pseudopotential based density functional theory as implemented in the CAMbridge Serial Total Energy Package (CASTEP) code [47,48]. The calculations setting are given below: The exchange and correlations terms: generalized gradient approximation (GGA) of the Perdew–Burke–Ernzerhof (PBE) [49]; cutoff energy: 500 eV; k-point [50] mesh: $10 \times 10 \times 3$; minimization technique: Broyden Fletcher Goldfarb Shanno (BFGS) [51]; electronic structure calculation: density mixing; energy convergence tolerance: 5×10^{-6} eV/atom; maximum force tolerance: 0.01 eV/Å; maximum ionic displacement tolerance: 5×10^{-4} Å; and maximum stress tolerance: 0.02 GPa. The pseudo-atomic calculations were performed for B - $2s^2 2p^1$, Pb- $5d^{10} 6s^2 6p^2$, Bi - $6s^2 6p^3$, and Hf - $5d^2 6s^2$ electronic orbitals.

3. Results and discussion

3.1. Structural properties

The characteristic unit cell for 211 MAX phases is shown in Fig. 1, crystallized with hexagonal structure [Space group P63/mmc][1]. The Hf_2AB ($A = \text{Pb, Bi}$) borides belong to the 211 subclass of MAX phases, therefore, the Hf_2AB ($A = \text{Pb, Bi}$) has the same unit cell characteristics except for the difference in the lattice constants and internal parameter. The atomic positions of Hf, Pb/Bi and B atoms in the unit cell are $(1/3, 2/3, z_M)$, $(1/3, 2/3, 3/4)$ and $(0, 0, 0)$, respectively. The values of the internal parameter, z_M are given in Table 1. The optimized lattice constants (a , c), internal parameter and c/a ratio of Hf_2AB ($A = \text{Pb and Bi}$) are listed in Table 1 along with the

reported results for comparison. As seen in Table 1 that the calculated values of a and c are very close to the reported values. A very low deviation from the available theoretical values certifies the accuracy of the present calculations. No experimental values are available for comparison since these phases are not synthesized yet.

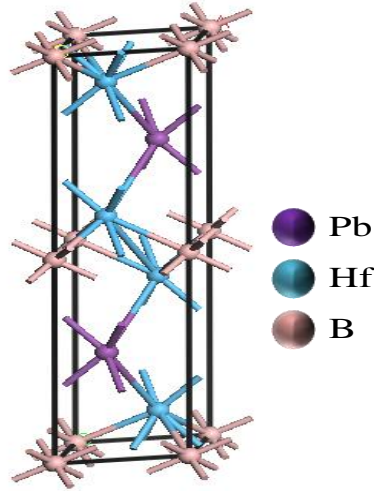


Fig. 1 - Crystal structure of the Hf_2PbB compound.

Table 1 Calculated lattice parameters (a and c), internal parameter (z_M) and c/a ratio of Hf_2AB (A = Pb, Bi) MAX phases.

Table 1 Calculated lattice parameters (a and c), internal parameter (z_M) and c/a ratio of Hf_2AB (A = Pb, Bi) MAX phases.

Phase	a (Å)	% of deviation	c (Å)	% of deviation	z_M	c/a	Reference
Hf_2PbB	3.493	0.721	14.899	0.454	0.0840	4.267	This work
	3.468		14.967		0.0826	4.316	[46]
Hf_2BiB	3.530	0.199	14.374	0.794	0.0867	4.07	This work
	3.523		14.489		0.0826	4.113	[46]

3.2 Mechanical properties

To explore the mechanical behavior of Hf_2AB (A = Pb, Bi) MAX phases, we have calculated the mechanical properties characterizing parameters using the strain-stress method [41,52–54] as implement in the CASTEP code. Before starting with the mechanical properties, the mechanical

stability of Hf₂AB (A = Pb, Bi) should be checked by employing well known stability conditions for the hexagonal system based on the stiffness constants (C_{ij}). The obtained stiffness constants satisfies the following conditions [55,56]: $C_{11} > 0$, $C_{33} > 0$, $C_{44} > 0$, $C_{11} - C_{12} > 0$, $(C_{11} + C_{12})C_{33} - 2C_{13}^2 > 0$; hence the Hf₂AB (A = Pb, Bi) MAX members are mechanically stable. The obtained stiffness constants are compared with those of other Hf-based [Hf₂AB (A = Al, Ga, In, S)] borides as shown in Fig. 2 (a). It is seen that the stiffness constants of Hf₂AB (A = Pb, Bi) are lower than those of Hf₂AB (A = Al, S) borides but higher than those of Hf₂AB (A = Ga, In) borides. The obtained values are also presented in Table 2 for an easy understanding of the exact values. It is well known that the C_{11} and C_{33} measure the stiffness of solids along a and c -axis, therefore, the differences in the values of C_{11} and C_{33} indicating the anisotropic nature of the bonding strength. It is also observed that for the Hf₂PbB, $C_{11} > C_{33}$, indicating stiffer nature along a -axis compared to c -axis like Hf₂AB (A = Ga, In) borides whereas for the Hf₂BiB, $C_{11} < C_{33}$, indicating stiffer nature along the c -axis compared to a -axis like Hf₂AB (A = Al, S) borides [38,44]. Moreover, these stiffness constants are further used to calculate the polycrystalline elastic moduli using well-known formalisms. For example, the bulk modulus (B) and shear modulus (G) are calculated using Hill's approximation [57,58] that usually expressed the average values of the upper limit (Voigt [59]) and lower limit (Reuss [60]) of B : [$B = (B_V + B_R)/2$] and G : [$G = (G_V + G_R)/2$]. The B_V , B_R , G_V and G_R are calculated from C_{ij} using the following equations: $B_V = [2(C_{11} + C_{12}) + C_{33} + 4C_{13}]/9$; $B_R = C^2/M$; $C^2 = C_{11} + C_{12})C_{33} - 2C_{13}^2$; $M = C_{11} + C_{12} + 2C_{33} - 4C_{13}$; $G_V = [M + 12C_{44} + 12C_{66}]/30$ and $G_R = (\frac{5}{2}) [C^2 C_{44} C_{66}] / [3B_V C_{44} C_{66} + C^2 (C_{44} + C_{66})]$; $C_{66} = (C_{11} - C_{12})/2$. The Young's modulus and Poisson's ratio are also calculated from the B and G using the relations: $Y = 9BG/(3B + G)$ and $\nu = (3B - Y)/(6B)$ [61,62]. The elastic moduli (B , G , Y) of Hf₂AB (A = Pb, Bi) are higher than those of Hf₂AB (A = Ga, In) but lower than those of Hf₂AB (A = Al, S); are not directly related to the hardness of solids but these moduli are higher for harder solids. Therefore, the hardness of Hf₂AB (A = Pb, Bi) is expected to be lower than that of Hf₂AB (A = Al, S) but higher than that of Hf₂AB (A = Ga, In). One of the ways of comparing hardness is the calculations of hardness parameters H_{macro} and H_{micro} for compounds having a similar structure [63].

Table 2 The elastic constants, C_{ij} (GPa), bulk modulus, B (GPa), shear modulus, G (GPa), Young's modulus, Y (GPa), micro hardness, H_{micro} (GPa), macro hardness, H_{macro} (GPa), Pugh ratio, G/B , and Poisson ratio, ν , of Hf_2AB ($A = \text{Pb, Bi}$), together with those of Hf_2AB ($A = \text{Al, Ga, In, S}$) for comparison.

Phase	C_{11}	C_{12}	C_{13}	C_{33}	C_{44}	B	G	Y	H_{macro}	H_{micro}	G/B	ν	Reference
Hf_2PbB	225	58	51	206	75	108	76	192	15.01	15.63	0.73	0.21	This work
Hf_2BiB	206	66	70	212	82	115	72	184	11.94	13.20	0.67	0.23	This work
Hf_2AlB	232	72	81	267	109	133	92	223	15.31	17.14	0.69	0.22	[44]
Hf_2GaB	213	77	63	176	66	111	67	167	9.96	11.20	0.60	0.25	[44]
Hf_2InB	210	69	50	197	55	106	65	163	9.97	11.11	0.61	0.25	[44]
Hf_2SB	285	81	92	298	130	156	112	271	18.45	21.63	0.72	0.21	[38]

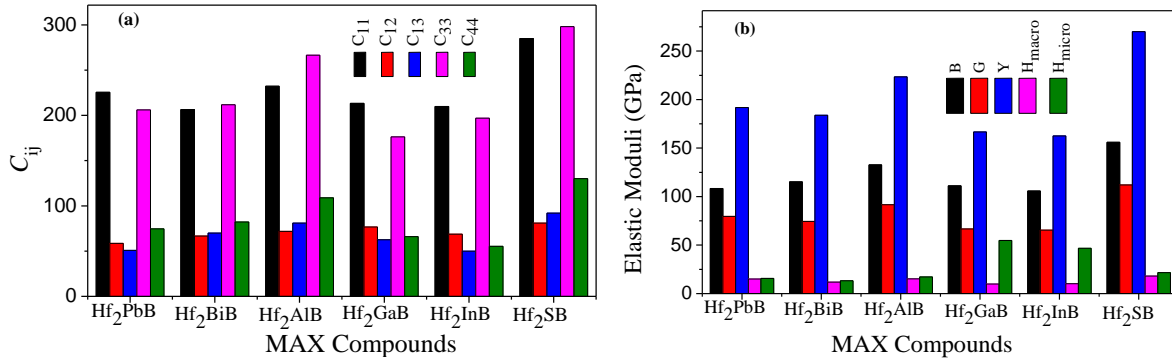


Fig. 2 Comparison of (a) C_{ij} and (b) B , G , Y , H_{macro} and H_{micro} of Hf_2AB ($A = \text{Pb, Bi}$) with those of Hf_2AB ($A = \text{Al, Ga, In, S}$).

To do this, we have used the elastic moduli further to calculate the hardness parameters using the equations: $H_{\text{macro}} = 2\left[\left(\frac{G}{B}\right)^2 G\right]^{0.585} - 3$ [64,65] and $H_{\text{micro}} = \frac{(1-2\nu)Y}{6(1+\nu)}$ [66]. These two equations expressed the role of elastic moduli to the hardness of solids; G is more related to the H_{macro} compared to B while Y is directly related to the H_{micro} . Fig. 2 (b) shows a comparison among the elastic moduli and hardness parameters of Hf_2AB ($A = \text{Pb, Bi}$) together with those of Hf_2AB ($A = \text{Al, Ga, In, S}$) MAX phase borides. Like C_{ij} , the elastic moduli and hardness parameters of Hf_2AB ($A = \text{Pb, Bi}$) are lower than those of Hf_2AB ($A = \text{Al, S}$) borides but higher than those of Hf_2AB ($A = \text{Ga, In}$) borides. The values are also presented in Table 2 for an easy understanding of the exact values. Though the hardness parameters are larger for the Hf_2PbB compared to the Hf_2BiB but the C_{44} of Hf_2BiB (82 GPa) is slightly larger than that of Hf_2PbB (75 GPa). Among the mechanical properties characterizing parameters, C_{44} is the best hardness predictor as

suggested by Jhi *et al.*[67] based on the results for binary carbides and nitrides. Therefore, the hardness should be higher for the Hf₂BiB compared to the Hf₂PbB. Actually, these hardness parameters do not predict exact hardness but efficient to predict comparative hardness based on the values of elastic moduli which are usually higher for harder solids. In order to predict the hardness more exactly, we have calculated the Vickers hardness (H_v) using the formula proposed by Gou *et al.*[68] for partial metallic solids. The detail of the formalism can be found elsewhere [69–72]. The important feature of this method is that it is the geometrical averages of all bonds present in the solids. The calculated Vickers hardness of Hf₂AB (A = Pb, Bi) is presented in Table 3. As seen in Table 3, the H_v of the Hf₂BiB (2.85 GPa) is slightly higher than that of Hf₂PbB (2.56 GPa), in good agreement with the Jhi *et al.*[67] statement.

Table 3 Calculated Mulliken bond number n^μ , bond length d^μ , bond overlap population P^μ , metallic population $P^{\mu'}$, bond volume v_b^μ , bond hardness H_v^μ of μ -type bond and Vickers hardness H_v of Hf₂AB (A = Pb, Bi).

Compounds	Bond	n^μ	d^μ (Å)	P^μ	$P^{\mu'}$	v_b^μ (Å ³)	H_v^μ (GPa)	H_v (GPa)
Hf ₂ PbB	Hf-B	4	2.37382	1.68	0.1028	39.367	2.56	2.56
Hf ₂ BiB	Hf-B	4	2.38886	1.73	0.0175	38.781	2.85	2.85

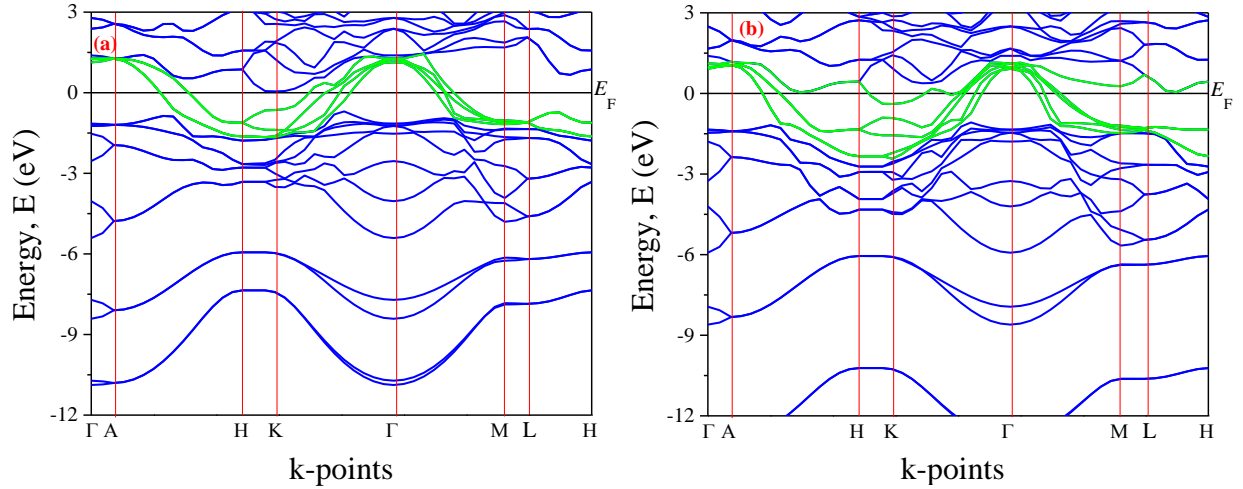
The difference in the values of Vickers hardness, in other words the bonding strength can be explain in terms of density of states (DOS) that will be presented in the 3.3 section.

The brittleness of Hf₂AB (A = Pb, Bi)

The most interesting characteristic of MAX phases is the extraordinary combinations of properties of metals and ceramics [3]. Like metals, they are machinable as discussed in the previous section; they are also brittle like ceramic materials. The brittleness of Hf₂AB (A = Pb, Bi) is evaluated by the Pugh ratio (G/B) and Poisson's ratio (ν). The calculated values of G/B and ν are listed in Table 2. A critical value of 0.571 for G/B [73] is considered as a borderline for ductile to brittle transition whereas the critical value of ν is 0.26 [74] that fixed the brittle-ductile borderline. As seen in Table 2 that the $G/B > 0.572$ and $\nu < 0.26$, thus, the Hf₂AB (A = Pb, Bi) are fall into the brittle class of materials.

3.3 Electronic Properties

The detail of the electronic nature of Hf_2AB ($A = \text{Pb, Bi}$) can be explained by exploring the electronic band structure and density of states (DOS) (total and partial). The electronic band structures of Hf_2AB ($A = \text{Pb, Bi}$) is shown in Fig. 3 (a and b). The Fermi level is set at zero of the energy scale. As seen from the figures that no band gap is appeared owing to the overlapping of the valence band and conduction band. Consequently, metallic nature is exhibited by the MAX phase borides [Hf_2AB ($A = \text{Pb, Bi}$)]. Moreover, the anisotropic nature in electronic conductivity is also exhibited by the band structure of Hf_2AB ($A = \text{Pb, Bi}$) borides. The paths Γ -A, H-K and M-L exhibit the energy dispersion in the c -direction whereas the paths A-H, K- Γ , Γ -M and L-H exhibit energy dispersion in the basal planes. As observed from Fig 3, the degree of energy dispersion is lesser along the c -direction compared to the basal plane [75] owing to the higher effective mass tensor for conduction along c -direction than that of the basal plane (ab -plane) [76].



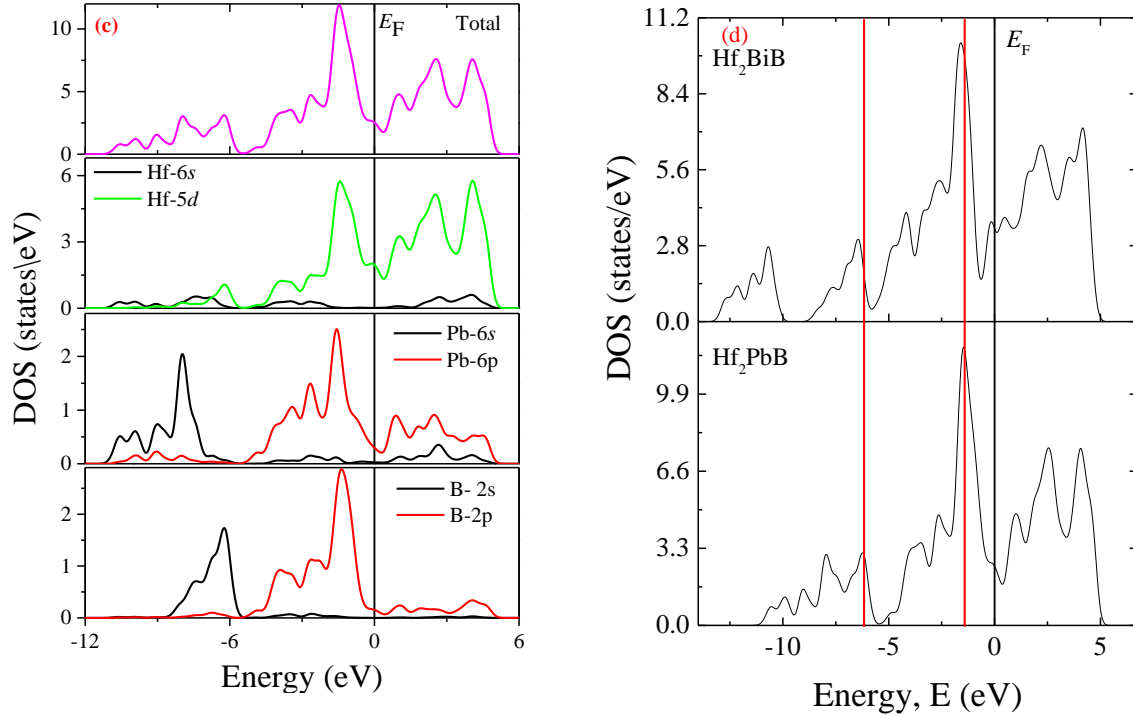


Fig. 3 Electronic band structure (a) Hf₂PbB and (b) Hf₂BiB; (c) total and partial DOS of Hf₂PbB; (d) total DOS of Hf₂AB (A = Pb and Bi) MAX phases.

To evaluate the contribution from the different electronic states to the electronic conductivity we have also calculated the total and partial DOS of Hf₂AB (A = Pb, Bi) borides. Owing to the similar nature except for the differences in the position of the peaks [can be understood from the position of the curves in band structures shown in Fig. 3 (a and b)] only the total and partial DOS of Hf₂PbB is presented in Fig. 3 (c). As seen in the figure that the prime contribution comes from the Hf-5*d* states to the DOS at the Fermi level while Pb-6*p* and B-2*p* also contribute but lesser in magnitude compared to the Hf-5*d* orbital. The partial DOS is also an effective tool to disclose the hybridization among the different states. The valence band can be divided into energy ranges: - 12.0 eV to -6.0 eV and -6.0 eV to - 0.0 eV. The Pb-6*s* and B-2*s* hybridized strongly that lead the peaks in the low energy region of the total DOS. The energy region of 0 eV to -6 eV is dominated by Hf-5*d* which is also hybridized with the Pb-6*p* and B-2*p*.

The difference in the Vickers hardness can be explained with the help of DOS. For this reason, we have also calculated the DOS of Hf₂AB (A = Pb, Bi) as shown in Fig. 3 (d) in which a black

solid line refers to the Fermi level and two solid red lines are used to demonstrate the shifting of peaks in the DOS. As observed in Fig. 3 (d), the positions of the peaks are slightly shifted to the left (low energy side) for the Hf₂BiB phase. The peaks in the DOS are the consequence of the hybridization between different orbitals and the peak's position defines the energy of the hybridized states. The energy measures the strength of the hybridization, consequently, the bonding strength between unlike atoms. In general, the lower position of the peaks, the higher strength of the bonds [76]. Therefore, stronger bonding between unlike atoms is expected for the Hf₂BiB compared to the Hf₂PbB as consistent from the values of C_{44} (Table 2) and Vickers hardness (Table 3).

3.3 The elastic anisotropy

In Table 2, it is observed that $C_{11} > C_{33}$ for the Hf₂PbB and $C_{11} < C_{33}$ for the Hf₂BiB. These unequal values confirm the anisotropic nature of the mechanical properties because other parameters such as different polycrystalline elastic moduli are calculated from the stiffness constants C_{ij} . This aspect encouraged us to investigate mechanical anisotropy because some physical processes are greatly influenced by the anisotropic nature of elastic moduli [77]. Moreover, the study of anisotropy provides the information required to improve the stability of solids for many applications [78]. Thus, the anisotropic nature of Hf₂AB (A = Pb, Bi) is investigated considering different formalisms. At first, we investigate the different anisotropic factors directly related to the stiffness constants. For example, the shear anisotropic factors for the {100}, {010} and {001} planes is computed using the equations:

$$A_1 = \frac{1/6(C_{11}+C_{12}+2C_{33}-4C_{13})}{C_{44}}, A_2 = \frac{2C_{44}}{C_{11}-C_{12}}, A_3 = A_1 \cdot A_2 = \frac{1/3(C_{11}+C_{12}+2C_{33}-4C_{13})}{C_{11}-C_{12}} \quad [79],$$

respectively and presented in Table 4. As observed in Table 4, the values of A_i 's are not equal to 1 (one). $A_i = 1$, implies the isotropic nature, thus, the compounds in interest are anisotropic ($A_i \neq 1$). The unequal values of bulk modulus along a and c -axis are estimated by the following equations

$$[80]: B_a = a \frac{dP}{da} = \frac{\Lambda}{2+\alpha}, B_c = c \frac{dP}{dc} = \frac{B_a}{\alpha}, \text{ where } \Lambda = 2(C_{11} + C_{12}) + 4C_{13}\alpha + C_{33}\alpha^2 \text{ and } \alpha = \frac{(C_{11}+C_{12})-2C_{13}}{C_{33}+C_{13}}.$$

The values of B_a and B_c are not equal, which implies the anisotropy of Hf₂AB (A = Pb, Bi). The linear compressibility (k) are different along the a and c -axis. Their ratio is estimated by the following relation[81]: $\frac{k_c}{k_a} = C_{11} + C_{12} - 2C_{13} / (C_{33} - C_{13})$. A value of $k_c/k_a =$

1, implies the isotropic nature of solids, thus, $k_c/k_a \neq 1$ (Table 4) for compounds in interests indicating the anisotropy of Hf₂AB (A = Pb, Bi).

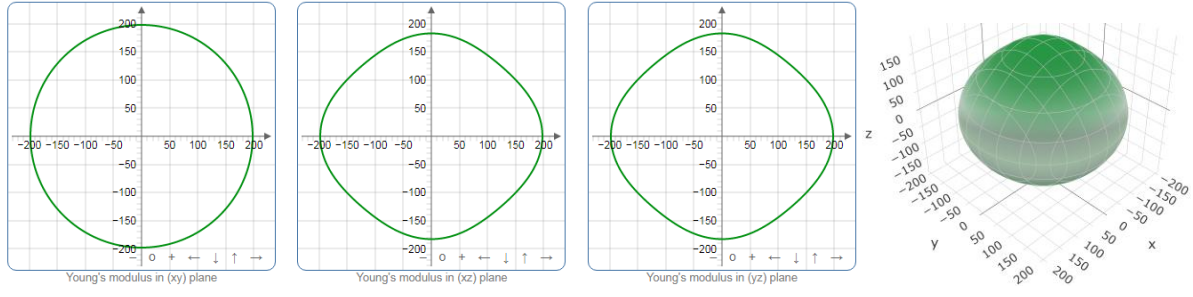
Table 4 Anisotropic factors, $A_1, A_2, A_3, k_c/k_a, B_a, B_c$, percentage anisotropy factors A_G and A_B , and universal anisotropic index A^U of Hf₂AB (A = Pb, Bi), together with those of the Hf₂AB (A = Al, Ga, In and S) for comparison.

<i>Phase</i>	A_1	A_2	A_3	B_a	B_c	k_c/k_a	A_B	A_G	A^U	<i>References</i>
Hf ₂ PbB	1.10	0.89	1.01	301	424	1.172	0.156	0.163	0.019	This work
Hf ₂ BiB	0.84	1.17	0.99	293	620	0.94	0.017	0.322	0.033	This work
Hf ₂ AlB	0.79	1.36	1.07	366	479	0.76	0.021	0.017	0.480	[44]
Hf ₂ GaB	0.98	0.97	0.96	381	263	1.45	0.023	0.018	0.572	[44]
Hf ₂ InB	1.43	0.78	1.12	340	279	1.22	0.024	0.023	0.711	[44]
Hf ₂ SB	0.76	1.27	0.97	447	506	0.88	0.067	0.788	0.080	[38]

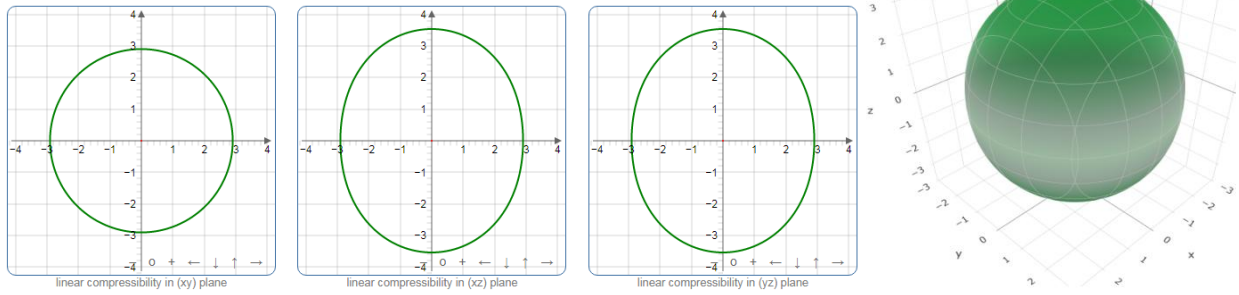
Anisotropy is attributed due to the differences in the values of bulk modulus and shear modulus obtained using Voigt and Reuss models. This anisotropy is calculated using the formulae: $A_B = \frac{B_V - B_R}{B_V + B_R} \times 100\%$ and $A_G = \frac{G_V - G_R}{G_V + G_R} \times 100\%$ [82]. The universal anisotropic index A^U is computed using the equation based on the obtained values of B and G using Voigt and Reuss models [83]: $A^U = 5 \frac{G_V}{G_R} + \frac{B_V}{B_R} - 6 \geq 0$. The zero values of A_B, A_G and A^U define the solid as isotropic otherwise anisotropic materials. Thus, the non-zero values of the mentioned parameters (Table 4) imply that the compounds under consideration are anisotropic.

In addition, we have also investigated the anisotropy in elastic moduli of Hf₂AB (A = Pb, Bi) such as Young's modulus (Y), linear compressibility ($K=1/B$), shear modulus (G) and Poisson's ratio (ν) by presenting their values in 2D and 3D. The 2D and 3D plots are presented in Fig. 4(a-d) for the Hf₂PbB and Fig. 5 (a-d) for the Hf₂BiB phase that have been created using the ELATE code [84,85] based on their stiffness matrix.

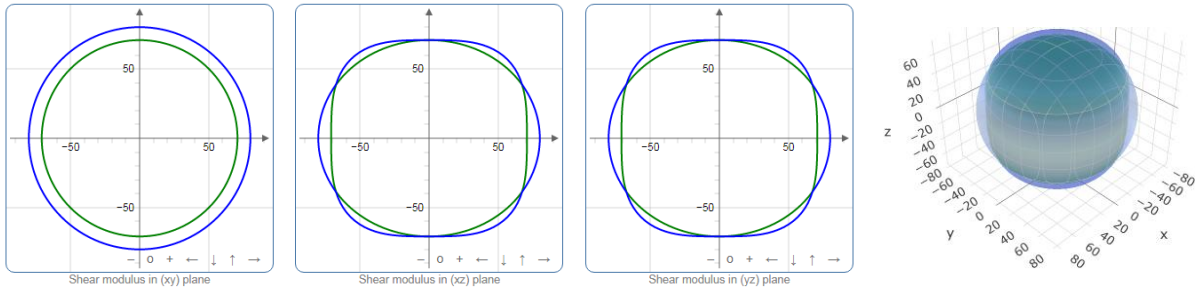
(a) Young's modulus (Y),



(b) Linear compressibility ($K=1/B$)



(c) Shear modulus (G)



(d) Poisson's ratio (ν)

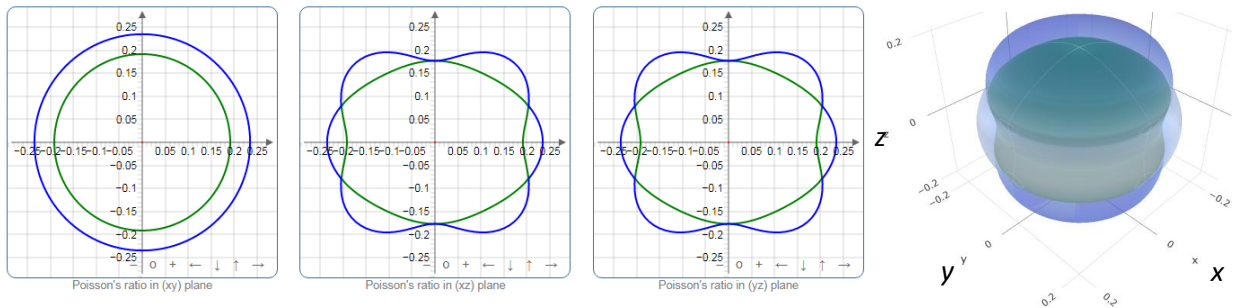
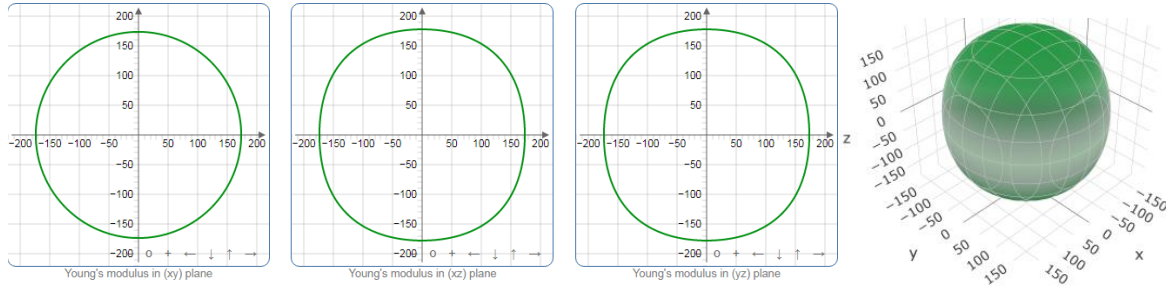
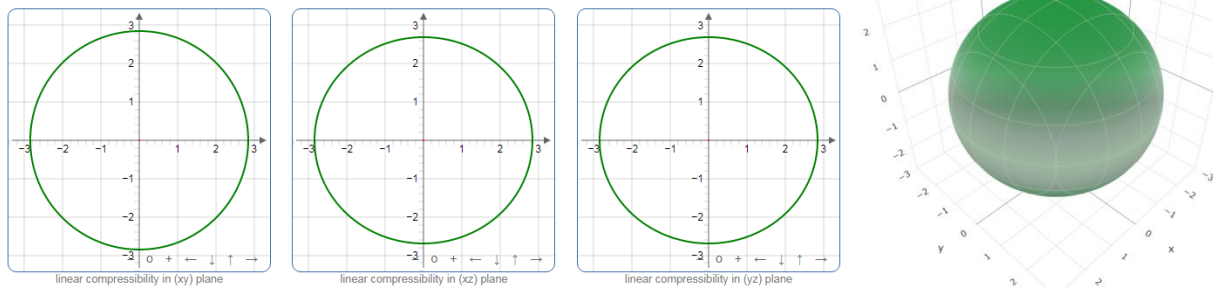


Fig. 4: The 2D and 3D plots of (a) Y , (b) K , (c) G and (d) ν of the Hf_2PbB compound.

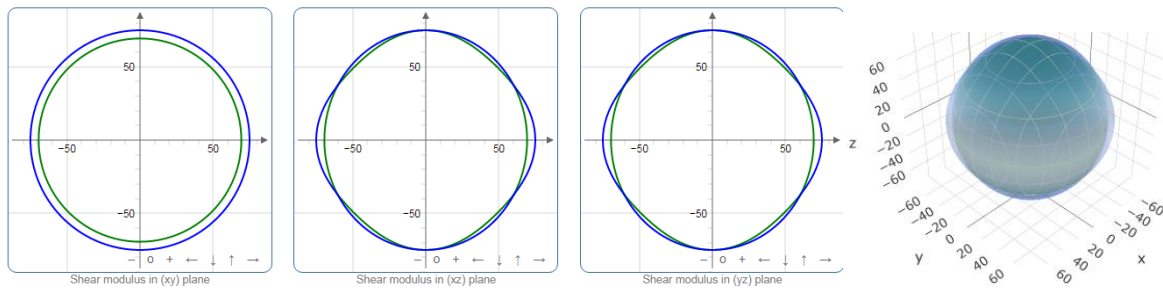
(a) Young's modulus (Y),



(b) Linear compressibility ($K=1/B$)



(c) Shear modulus (G)



(d) Poisson's ratio (ν)

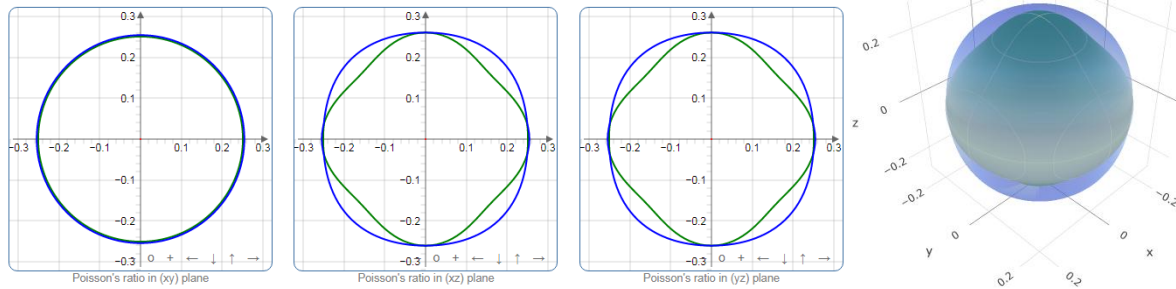


Fig. 5: The 2D and 3D plots of (a) Y , (b) K , (c) G and (d) ν of the Hf_2BiB compound.

A perfect circle/sphere represents an isotropic solids and vice versa. The anisotropy level can be understood from the deviation of circular (for 2D) and spherical (for 3D) presentation of the

elastic moduli. For example, comparatively a greater extent of deviation from circle or sphere is observed for the Hf₂PbB compared to Hf₂BiB, suggesting a more anisotropic nature as seen from values of A_Y , A_K , A_G , A_v in Table 5. 2D plots of elastic moduli help to understand the anisotropic nature exhibited by 3D plots. For example, it is seen in 2D plots of Y that the Hf₂PbB phase has a maximum value of Y at the horizontal axis in both xz and yz planes which is to be isotropic in xy plane while the Hf₂BiB phase has the maximum value of Y at an angle of 45° in between the axes. The compressibility is maximum along the vertical axis of both xz and yz planes for the Hf₂PbB while it is maximum along the horizontal axis in both xz and yz planes for the Hf₂BiB. The shear modulus is minimum at both axes in both xz and yz planes for the Hf₂PbB while it is maximum at the vertical axes in both xz and yz planes for the Hf₂BiB. The Poisson's ratio also exhibits different anisotropy for both compounds. It is minimum at both axes in both xz and yz planes for the Hf₂PbB phase but maximum at both axes in both xz and yz planes for the Hf₂BiB phase. A common thing is present for the compounds; all the elastic moduli are to be isotropic in xy plane.

Table 5: The minimum and the maximum values of the Young's modulus, compressibility, shear modulus, and Poisson's ratio of Hf₂AB (A = Pb, Bi).

Phase	$Y_{\min.}$ (GPa)	$Y_{\max.}$ (GPa)	A_Y	K (TPa^{-1})	K (TPa^{-1})	A_K	$G_{\min.}$ (GPa)	$G_{\max.}$ (GPa)	A_G	$\nu_{\min.}$	$\nu_{\max.}$	A_v
Hf ₂ PbB	182.95	203.05	1.11	2.909	3.419	1.17	74.66	83.49	1.12	0.179	0.233	1.30
Hf ₂ BiB	173.01	193.07	1.12	2.774	2.952	1.06	69.58	82.19	1.18	0.174	0.273	1.57

3.3 Thermal properties

MAX phases have good mechanical properties at high temperature that makes them potentials candidates for high-temperature technology. Thus, the dissemination of knowledge regarding the high-temperature application is of scientific interest. This can be done by evaluating thermal properties characterizing parameters such as Debye temperature (Θ_D), minimum thermal conductivity (K_{\min}) and Grüneisen parameter (γ) and so on. In this study, we have calculated Θ_D , K_{\min} and γ of Hf₂AB (A = Pb, Bi) and tried to correlate with the mechanical properties for the same. The thermal properties characterizing parameters of Hf₂AB (A = Al, Ga, In) are also calculated using published data. The Debye temperature (Θ_D) is considered as a fundamental thermal parameter that can link the mechanical properties of solids with other important physical

processes [70,76,86]. Anderson's method [87] is widely used [63,69,70,72,88] and very simple to calculate the Θ_D by calculating the sound velocities passing through the solids. The equation used in this calculation is the following: $\Theta_D = \frac{h}{k_B} \left[\left(\frac{3n}{4\pi} \right) N_A \rho / M \right]^{1/3} v_m$, where, M be the molar mass, n be the number of atoms in the molecules, ρ be the mass density, and h , k_B , and N_A be the Plank's constant, Boltzmann constant and Avogadro's number, respectively. The v_m is the mean sound velocity that is obtained by the formula: $v_m = \left[\frac{1}{3} (v_l^3 + 2v_t^3) \right]^{-1/3}$ where, v_l and v_t are the velocity of sound for longitudinal and transverse mode, respectively. The v_l and v_t are estimated using the following equations: $v_l = [(3B + 4G)/3\rho]^{1/2}$ and $v_t = [G/\rho]^{1/2}$. The obtained values of density, longitudinal, transverse and average sound velocities (v_l , v_t , and v_m , respectively) and the Θ_D of Hf₂AB (A = Pb, Bi) are presented in Table 6. The Θ_D of Hf₂AB (A = Pb, Bi) is close to each other like their mechanical properties characterizing parameters. Though the Vickers hardness of the Hf₂BiB is lightly higher than that of Hf₂PbB, thus, higher Θ_D for the Hf₂BiB compound is expected. But, the Θ_D for the Hf₂BiB is slightly smaller than that of the Hf₂PbB. The reason might be that the atomic mass of Bi is higher than that of Pb that leads to a higher density of the Hf₂BiB, results a lower Θ_D value for the Hf₂BiB compared to Hf₂PbB [72]. The inverse role of density can be seen in the formulae used to calculate the Θ_D . The values of v_l , v_t , and v_m are also in agreement with our explanation. The Θ_D values for other Hf-based 211 borides presented here are in well consistent with our assumption.

Minimum thermal conductivity (K_{min}) becomes one of the fundamental parameters for materials which are used at high-temperature application, thus, the study of K_{min} of MAX phase materials is of scientific importance because of their usefulness in the high-temperature technology. The thermal conductivity of materials (e.g., ceramics) downs to a constant value (K_{min}) at high temperatures. The K_{min} of Hf₂AB (A = Pb, Bi) has been estimated using the equation [89]: $K_{min} = k_B v_m \left(\frac{M}{n\rho N_A} \right)^{-2/3}$, where k_B , v_m , N_A and ρ are Boltzmann constant, average phonon velocity, Avogadro's number and density of crystal, respectively and presented in Table 6. The reported values of K_{min} for the compounds are also given in Table 6 that are comparable with that of other MAX phases [30,90]. The values are close to each other for the compound, revealing the usefulness of Hf₂AB (A = Pb, Bi) as an alternative of Hf₂AB (A = Al, Ga, In and S) compounds for desired applications.

Table 6 Calculated density (ρ), longitudinal, transverse and average sound velocities (v_l , v_t , and v_m , respectively), Debye temperature (Θ_D), minimum thermal conductivity (K_{\min}) and Grüneisen parameter (γ) of Hf_2AB ($A = \text{Pb, Bi}$) borides, together with those of the Hf_2AB ($A = \text{Al, Ga, In}$ and S) for comparison.

Phase	ρ (g/cm ³)	v_l (m/s)	v_t (m/s)	v_m (m/s)	Θ_D (K)	K_{\min} (W/mK)	γ	Reference
Hf_2PbB	12.12	4145	2504	2768	305	0.796	1.19	This work
Hf_2BiB	12.33	4175	2416	2681	297	0.778	1.33	This work
Hf_2AlB	9.10*	5301*	3180*	3518*	399*	0.866#	1.49*	This work
Hf_2GaB	10.26*	4417*	2557*	2836*	324*	0.713#	1.36*	This work
Hf_2InB	10.43*	4297*	2496*	2769*	308*	0.661#	1.50*	This work
Hf_2SB	10.19	5465	3309	3657	430	0.792	1.50	[38]

*Calculated using published data, #Ref-[44]

The Grüneisen parameter (γ) is an important thermal parameter from which the anharmonic effects owing to the lattice dynamics can be understood. We have calculated the γ for Hf_2AB ($A = \text{Pb, Bi}$) compounds using the following relationship between γ and ν [91]: $\gamma = \frac{3}{2} \frac{(1+\nu)}{(2-3\nu)}$. The γ for Hf_2AB ($A = \text{Al, Ga}$ and In) have also been calculated using the published data for comparison. As observed in Table 6, the computed values of γ are found to be in the range of .85 to 3.53 as expected for the polycrystalline materials having ν in the range of 0.05–0.46 [92]. Besides, quite low values of γ certify the low anharmonic effects within the compounds in interest. Moreover, the anharmonic effect is lesser in Hf_2AB ($A = \text{Pb, Bi}$) compounds compared to Hf_2AB ($A = \text{Al, Ga, In}$ and S) borides.

Although, the thermal expansion coefficient is still unknown but due to the low K_{\min} and considerably high melting temperature of Hf_2AB ($A = \text{Pb, Bi}$), it is expected that they could be potential candidates for thermal barrier coating (TBC) materials in high temperature technology.

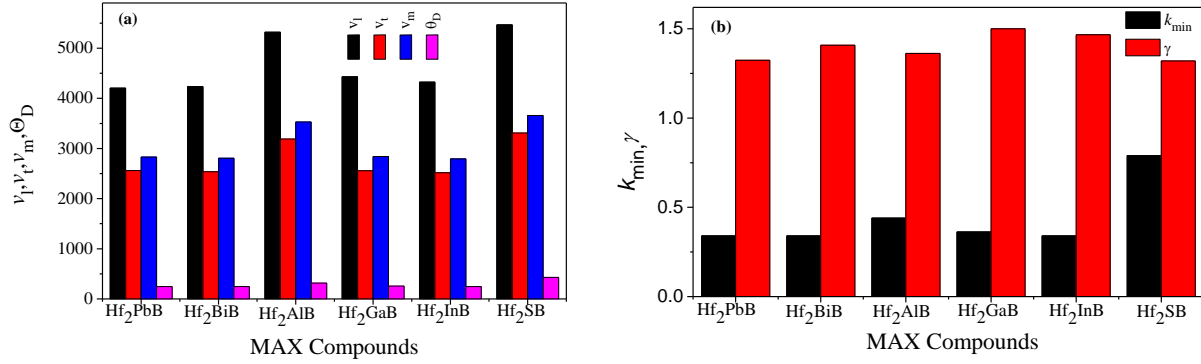


Fig. 6 Comparison of (a) sound velocities and Debye temperature and (b) minimum thermal conductivity and Grüneisen parameter of Hf₂AB (A = Pb, Bi) with those of Hf₂AB (A = Al, Ga, In, S).

3.6 Assessment of suitability as coating materials

One of the potential applications of the MAX phase materials is the use as outside layer materials to protect the inside from solar radiation. This sub-section is dedicated to evaluate the interaction between the electromagnetic (EM) radiation and studied materials. The interactions of EM ray and materials exhibit two physical phenomena: energy transformation (absorption, reflectivity and inelastic scattering) and propagation. Therefore, the present article intends to investigate the real component $\epsilon_1(\omega)$ and imaginary component $\epsilon_2(\omega)$ of dielectric function $\epsilon(\omega)$, where $\epsilon_2(\omega)$ exhibits absorption features of solids, directly related to the band structure of solids, whereas the real part $\epsilon_1(\omega)$ is important in the study of reflectivity and loss function, etc. The reflectivity and loss function can be obtained from $\epsilon_1(\omega)$ and $\epsilon_2(\omega)$. The detail of optical properties calculations can be found elsewhere [93–95].

The metallic nature of the studied MAX compounds is confirmed from the DOS as shown in Fig. 3. Thus, it is scientifically significant to correct the intra-band contribution to the imaginary part of the dielectric constants. To increase the low energy part of $\epsilon_2(\omega)$, a plasma frequency (3 eV) and a damping of 0.05 eV is introduced [96]. In addition, the obtained spectra have been broadened by the use of a Gaussian smearing (0.5 eV). The optical properties of Hf₂AB (A = Pb, Bi) are calculated up to 20 eV for both [100] and [001] direction to showcase the anisotropic nature and presented in Fig. 7. The optical anisotropy is clearly demonstrated by figures presented here for both polarization directions.

Fig. 7 (a) shows the $\epsilon_2(\omega)$ for both titled borides in which a clear difference is observed between the values for both directions. The both compounds exhibit almost identical spectra for [100] and [001] directions after 2.5 eV of incident photon energy. Fig. 7 (a) shows the $\epsilon_1(\omega)$ for both titled borides that has a large negative values for both directions. This is the Drude-like nature that confirms the metallic nature of compounds, in good agreement with band structure results.

The most important optical constant of MAX phase materials from application point of view is the reflectivity that is calculated [Fig. 7 (c)] to assess the suitability of the titled borides as cover materials to prevent the solar heating. Li *et al.* [95,96] have predicted the MAX phase materials for the same based on the values of reflectivity, they predicted that the materials with reflectivity 44% can be used as coating materials to reduce solar heating. As seen from Fig. 7 (c) that both compounds fulfill the above conditions. Thus, they can be used for the same as discussed here. The values of $R(0)$ for both [100] and [001] polarization directions of the electric field are 0.62 and 0.55 for Hf₂PbB; 0.66 and 0.51 for Hf₂BiB, respectively.

We have also calculated the loss function of Hf₂AB (A = Pb, Bi) compounds as shown in Fig. 7 (d). As this function signifies the energy loss of electrons during the propagation through the materials, therefore, the zero value of $L(\omega)$ up to certain energy indicates no energy loss of electrons. The peak observed at certain energy depicts the character of plasma oscillation and defines the characteristic frequency that is known as the plasma frequency ω_p of the material [97]. At ω_p , the real part of the dielectric function, $\epsilon_1(\omega)$, becomes positive from below when the $\epsilon_2(\omega) < 1$. The material exhibits dielectric response after ω_p . The ω_p for both [100] and [001] polarization directions are 13.4 eV and 14.2 eV for the Hf₂PbB; 13.7 eV and 14.9 eV for the Hf₂BiB, respectively, where a rapid decline of reflectivity is noticed.

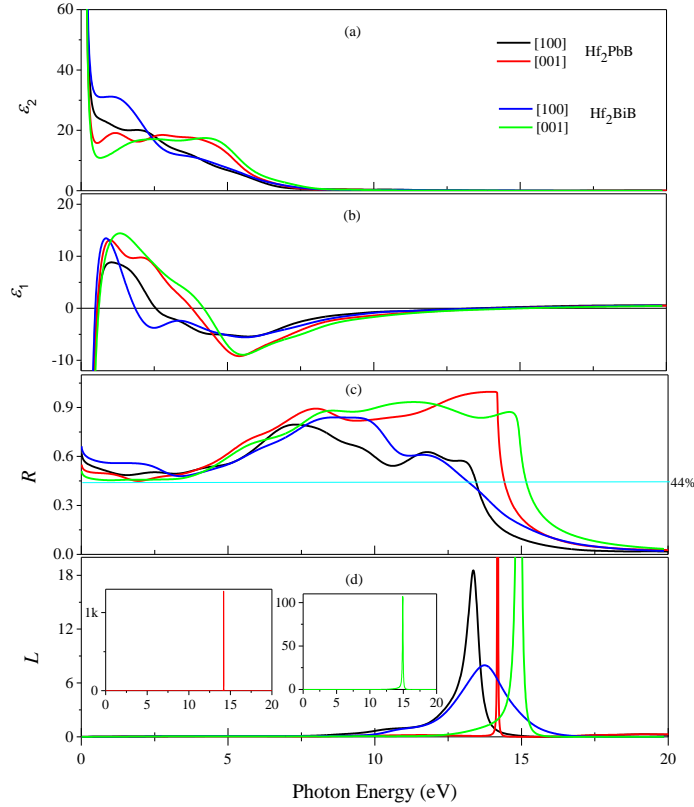


Fig. 7 The (a) real (ϵ_1), and (b) imaginary (ϵ_2) part of dielectric function, (c) reflectivity (R) and (d) loss function (L) of Hf₂AB (A = Pb, Bi) MAX phase borides.

4. Conclusions

In the present study, we have performed DFT calculations to explore the mechanical behavior including their anisotropic nature, electronic, thermal and optical properties of Hf₂AB (A = Pb, Bi) MAX phase borides. The obtained lattice constants agree well with prior reported values. The titled borides are mechanically stable as confirmed from the stability criteria using stiffness constants. The mechanical properties of Hf₂AB (A = Pb, Bi) are higher than those of Hf₂AB (A = Ga, In) but smaller than those of Hf₂AB (A = Al, S). The Vickers hardness of the Hf₂BiB phase is higher than that of the Hf₂PbB phase that is in good agreement with lower energy position of the peaks in the DOS. The titled materials are brittle in nature like other MAX phases materials. The electronic band structure and DOS imply that these materials are metallic in nature and anisotropic electronic conductivity is confirmed from different energy dispersion along different direction. The studied materials shows highly anisotropic in nature by calculating different anisotropic indexes and presenting 2D as well as 3D of Young's modulus, linear compressibility,

shear modulus and Poisson's ratio. The Debye temperature (Θ_D) of Hf_2AB ($A = \text{Pb, Bi}$) are found to be lower than that of other Hf based 211 MAX borides. The obtained minimum thermal conductivity of Hf_2AB ($A = \text{Pb, Bi}$) is very low, comparable to other MAX phase materials. A low anharmonic effects within the studied borides is confirmed from the values of Grüneisen parameter. The studied reflectivity spectra confirmed their possible use as cover materials to diminish solar radiation.

References

- [1] M.W. Barsoum, The $\text{MN}+1\text{AXN}$ phases: A new class of solids, *Prog. Solid State Chem.* 28 (2000) 201–281. [https://doi.org/10.1016/S0079-6786\(00\)00006-6](https://doi.org/10.1016/S0079-6786(00)00006-6).
- [2] M.W. Barsoum, *MAX phases: Properties of machinable ternary carbides and nitrides*, Wiley-VCH Verlag GmbH & Co. KGaA, Weinheim, Germany, 2013. <https://doi.org/10.1002/9783527654581>.
- [3] M. Radovic, M.W. Barsoum, MAX phases: Bridging the gap between metals and ceramics, *Am. Ceram. Soc. Bull.* 92 (2013) 20–27.
- [4] M.A. Ali, M.R. Khatun, N. Jahan, M.M. Hossain, Comparative study of $\text{Mo}_2\text{Ga}_2\text{C}$ with superconducting MAX phase Mo_2GaC : First-principles calculations, *Chinese Phys. B.* 26 (2017) 033102. <https://doi.org/10.1088/1674-1056/26/3/033102>.
- [5] F. Sultana, M.M. Uddin, M.A. Ali, M.M. Hossain, S.H. Naqib, A.K.M.A. Islam, First principles study of M_2InC ($M = \text{Zr, Hf and Ta}$) MAX phases: The effect of M atomic species, *Results Phys.* 11 (2018) 869–876. <https://doi.org/10.1016/j.rinp.2018.10.044>.
- [6] M.R. Khatun, M.A. Ali, F. Parvin, A.K.M.A. Islam, Elastic, thermodynamic and optical behavior of V_2AC ($A = \text{Al, Ga}$) MAX phases, *Results Phys.* 7 (2017) 3634–3639. <https://doi.org/10.1016/j.rinp.2017.09.043>.
- [7] A. Chowdhury, M.A. Ali, M.M. Hossain, M.M. Uddin, S.H. Naqib, A.K.M.A. Islam, Predicted MAX Phase Sc_2InC : Dynamical Stability, Vibrational and Optical Properties, *Phys. Status Solidi.* 255 (2017) 1700235. <https://doi.org/10.1002/pssb.201700235>.
- [8] M.A. Ali, M.T. Nasir, M.R. Khatun, A.K.M.A. Islam, S.H. Naqib, An *ab initio* investigation of vibrational, thermodynamic, and optical properties of Sc_2AlC MAX compound, *Chinese Phys. B.* 25 (2016) 103102. <https://doi.org/10.1088/1674-1056/25/10/103102>.
- [9] M.A. Rayhan, M.A. Ali, S.H. Naqib, A.K.M.A. Islam, First-principles Study of Vickers Hardness and Thermodynamic Properties of Ti_3SnC_2 Polymorphs, *J. Sci. Res.* 7 (2015) 53–64. <https://doi.org/10.3329/jsr.v7i3.23182>.
- [10] P. Chakraborty, A. Chakrabarty, A. Dutta, T. Saha-Dasgupta, Soft MAX phases with boron substitution: A computational prediction, *Phys. Rev. Mater.* 2 (2018) 103605.

<https://doi.org/10.1103/PhysRevMaterials.2.103605>.

- [11] M. Sokol, V. Natu, S. Kota, M.W. Barsoum, On the Chemical Diversity of the MAX Phases, *Trends Chem.* 1 (2019) 210–223. <https://doi.org/10.1016/j.trechm.2019.02.016>.
- [12] T. Lapauw, K. Lambrinou, T. Cabioch, J. Halim, J. Lu, A. Pesach, O. Rivin, O. Ozeri, E.N. Caspi, L. Hultman, P. Eklund, J. Rosén, M.W. Barsoum, J. Vleugels, Synthesis of the new MAX phase Zr₂AlC, *J. Eur. Ceram. Soc.* 36 (2016) 1847–1853. <https://doi.org/10.1016/j.jeurceramsoc.2016.02.044>.
- [13] T. Lapauw, J. Halim, J. Lu, T. Cabioch, L. Hultman, M.W. Barsoum, K. Lambrinou, J. Vleugels, Synthesis of the novel Zr₃AlC₂ MAX phase, *J. Eur. Ceram. Soc.* 36 (2016) 943–947. <https://doi.org/10.1016/j.jeurceramsoc.2015.10.011>.
- [14] M. Dahlqvist, J. Lu, R. Meshkian, Q. Tao, L. Hultman, J. Rosen, Prediction and synthesis of a family of atomic laminate phases with Kagomé-like and in-plane chemical ordering, *Sci. Adv.* 3 (2017) 1–10. <https://doi.org/10.1126/sciadv.1700642>.
- [15] H. Fashandi, C.C. Lai, M. Dahlqvist, J. Lu, J. Rosen, L. Hultman, G. Greczynski, M. Andersson, A. Lloyd Spetz, P. Eklund, Ti₂Au₂C and Ti₃Au₂C₂ formed by solid state reaction of gold with Ti₂AlC and Ti₃AlC₂, *Chem. Commun.* 53 (2017) 9554–9557. <https://doi.org/10.1039/c7cc04701k>.
- [16] M. Li, J. Lu, K. Luo, Y. Li, K. Chang, K. Chen, J. Zhou, J. Rosen, L. Hultman, P. Eklund, P.O.Å. Persson, S. Du, Z. Chai, Z. Huang, Q. Huang, Element Replacement Approach by Reaction with Lewis Acidic Molten Salts to Synthesize Nanolaminated MAX Phases and MXenes, *J. Am. Chem. Soc.* 141 (2019) 4730–4737. <https://doi.org/10.1021/jacs.9b00574>.
- [17] T. Lapauw, B. Tunca, T. Cabioch, J. Lu, P.O.Å. Persson, K. Lambrinou, J. Vleugels, Synthesis of MAX Phases in the Hf–Al–C System, *Inorg. Chem.* 55 (2016) 10922–10927. <https://doi.org/10.1021/acs.inorgchem.6b01398>.
- [18] B. Anasori, M. Dahlqvist, J. Halim, E.J. Moon, J. Lu, B.C. Hosler, E.N. Caspi, S.J. May, L. Hultman, P. Eklund, J. Rosén, M.W. Barsoum, Experimental and theoretical characterization of ordered MAX phases Mo₂TiAlC₂ and Mo₂Ti₂AlC₃, *J. Appl. Phys.* 118 (2015) 094304. <https://doi.org/10.1063/1.4929640>.
- [19] S. Kuchida, T. Muranaka, K. Kawashima, K. Inoue, M. Yoshikawa, J. Akimitsu, Superconductivity in Lu₂SnC, *Phys. C Supercond.* 494 (2013) 77–79. <https://doi.org/10.1016/j.physc.2013.04.050>.
- [20] Q. Xu, Y. Zhou, H. Zhang, A. Jiang, Q. Tao, J. Lu, J. Rosén, Y. Niu, S. Grasso, C. Hu, Theoretical prediction, synthesis, and crystal structure determination of new MAX phase compound V₂SnC, *J. Adv. Ceram.* 9 (2020) 481–492. <https://doi.org/10.1007/s40145-020-0391-8>.
- [21] M.S. Ali, M.A. Rayhan, M.A. Ali, R. Parvin, A.K.M.A. Islam, New MAX Phase Compound Mo₂TiAlC₂: First-principles Study, *J. Sci. Res.* 8 (2016) 109–117. <https://doi.org/10.3329/jsr.v8i2.25057>.

- [22] D. Horlait, S.C. Middleburgh, A. Chroneos, W.E. Lee, Synthesis and DFT investigation of new bismuth-containing MAX phases, *Sci. Rep.* 6 (2016) 1–9. <https://doi.org/10.1038/srep18829>.
- [23] E. Zapata-Solvas, M.A. Hadi, D. Horlait, D.C. Parfitt, A. Thibaud, A. Chroneos, W.E. Lee, Synthesis and physical properties of $(\text{Zr}_{1-x}, \text{Ti}_x)_3\text{AlC}_2$ MAX phases, *J. Am. Ceram. Soc.* 100 (2017) 3393–3401. <https://doi.org/10.1111/jace.14870>.
- [24] M. Naguib, G.W. Bentzel, J. Shah, J. Halim, E.N. Caspi, J. Lu, L. Hultman, M.W. Barsoum, New Solid Solution MAX Phases: $(\text{Ti}_{0.5}, \text{V}_{0.5})_3\text{AlC}_2$, $(\text{Nb}_{0.5}, \text{V}_{0.5})_2\text{AlC}$, $(\text{Nb}_{0.5}, \text{V}_{0.5})_4\text{AlC}_3$ and $(\text{Nb}_{0.8}, \text{Zr}_{0.2})_2\text{AlC}$, *Mater. Res. Lett.* 2 (2014) 233–240. <https://doi.org/10.1080/21663831.2014.932858>.
- [25] P.A. Burr, D. Horlait, W.E. Lee, Experimental and DFT investigation of $(\text{Cr}, \text{Ti})_3\text{AlC}_2$ MAX phases stability, *Mater. Res. Lett.* 5 (2017) 144–157. <https://doi.org/10.1080/21663831.2016.1222598>.
- [26] B. Tunca, T. Lapauw, O.M. Karakulina, M. Batuk, T. Cabioch, J. Hadermann, R. Delville, K. Lambrinou, J. Vleugels, Synthesis of MAX Phases in the Zr-Ti-Al-C System, *Inorg. Chem.* 56 (2017) 3489–3498. <https://doi.org/10.1021/acs.inorgchem.6b03057>.
- [27] T. Lapauw, B. Tunca, D. Potashnikov, A. Pesach, O. Ozeri, J. Vleugels, K. Lambrinou, The double solid solution $(\text{Zr}, \text{Nb})_2(\text{Al}, \text{Sn})\text{C}$ MAX phase: a steric stability approach, *Sci. Rep.* 8 (2018) 12801. <https://doi.org/10.1038/s41598-018-31271-2>.
- [28] B. Tunca, T. Lapauw, R. Delville, D.R. Neuville, L. Hennet, D. Thiaudière, T. Ouisse, J. Hadermann, J. Vleugels, K. Lambrinou, Synthesis and Characterization of Double Solid Solution $(\text{Zr}, \text{Ti})_2(\text{Al}, \text{Sn})\text{C}$ MAX Phase Ceramics, *Inorg. Chem.* 58 (2019) 6669–6683. <https://doi.org/10.1021/acs.inorgchem.9b00065>.
- [29] M. Griseri, B. Tunca, S. Huang, M. Dahlqvist, J. Rosén, J. Lu, P.O. Å. Persson, L. Popescu, J. Vleugels, K. Lambrinou, Journal of the European Ceramic Society Ta-based 413 and 211 MAX phase solid solutions with Hf and Nb, *J. Eur. Ceram. Soc.* 40 (2020) 1829–1838. <https://doi.org/10.1016/j.jeurceramsoc.2019.12.052>.
- [30] M.A. Ali, M.M. Hossain, M.A. Hossain, M.T. Nasir, M.M. Uddin, M.Z. Hasan, A.K.M.A. Islam, S.H. Naqib, Recently synthesized $(\text{Zr}_{1-x}\text{Ti}_x)_2\text{AlC}$ ($0 \leq x \leq 1$) solid solutions: Theoretical study of the effects of M mixing on physical properties, *J. Alloys Compd.* 743 (2018) 146–154. <https://doi.org/10.1016/j.jallcom.2018.01.396>.
- [31] R. Pan, J. Zhu, Y. Liu, Synthesis, microstructure and properties of $(\text{Ti}_{1-x}, \text{Mo}_x)_2\text{AlC}$ phases, *Mater. Sci. Technol.* 34 (2018) 1064–1069. <https://doi.org/10.1080/02670836.2017.1419614>.
- [32] O.O. Kurakevych, Superhard phases of simple substances and binary compounds of the B-C-N-O system: from diamond to the latest results (a Review), *J. Superhard Mater.* 31 (2009) 139–157. <https://doi.org/10.3103/S1063457609030010>.
- [33] P. Li, R. Zhou, X.C. Zeng, Computational Analysis of Stable Hard Structures in the Ti-B

- System, *ACS Appl. Mater. Interfaces*. 7 (2015) 15607–15617.
<https://doi.org/10.1021/acsami.5b04332>.
- [34] B. Feng, J. Zhang, Q. Zhong, W. Li, S. Li, H. Li, P. Cheng, S. Meng, L. Chen, K. Wu, Experimental realization of two-dimensional boron sheets, *Nat. Chem.* 8 (2016) 563–568.
<https://doi.org/10.1038/nchem.2491>.
- [35] J. Wang, M. Khazaei, M. Arai, N. Umezawa, T. Tada, H. Hosono, Semimetallic Two-Dimensional TiB₁₂: Improved Stability and Electronic Properties Tunable by Biaxial Strain, *Chem. Mater.* 29 (2017) 5922–5930.
<https://doi.org/10.1021/acs.chemmater.7b01433>.
- [36] T. Rackl, D. Johrendt, The MAX phase borides Zr₂SB and Hf₂SB, *Solid State Sci.* 106 (2020) 106316. <https://doi.org/10.1016/j.solidstatesciences.2020.106316>.
- [37] T. Rackl, L. Eisenburger, R. Niklaus, D. Johrendt, Syntheses and physical properties of the MAX phase boride Nb₂SB and the solid solutions Nb₂S_{1-x}B_x (x=0–1), *Phys. Rev. Mater.* 3 (2019) 054001. <https://doi.org/10.1103/PhysRevMaterials.3.054001>.
- [38] M.A. Ali, M.M. Hossain, M.M. Uddin, M.A. Hossain, A.K.M.A. Islam, S.H. Naqib, Physical properties of new MAX phase borides M₂SB (M = Zr, Hf and Nb) in comparison with conventional MAX phase carbides M₂SC (M = Zr, Hf and Nb): Comprehensive insights, (2020) 1–33. <http://arxiv.org/abs/2009.04236>.
- [39] J. Wang, T.N. Ye, Y. Gong, J. Wu, N. Miao, T. Tada, H. Hosono, Discovery of hexagonal ternary phase Ti₂InB₂ and its evolution to layered boride TiB, *Nat. Commun.* 10 (2019) 1–8. <https://doi.org/10.1038/s41467-019-10297-8>.
- [40] M.M. Ali, M.A. Hadi, I. Ahmed, A.F.M.Y. Haider, A.K.M.A. Islam, Physical properties of a novel boron-based ternary compound Ti₂InB₂, *Mater. Today Commun.* 25 (2020) 101600. <https://doi.org/10.1016/j.mtcomm.2020.101600>.
- [41] Y.X. Wang, Z.X. Yan, W. Liu, G.L. Zhou, Structure stability, mechanical properties and thermal conductivity of the new hexagonal ternary phase Ti₂InB₂ under pressure, *Philos. Mag.* 100 (2020) 2054–2067. <https://doi.org/10.1080/14786435.2020.1754485>.
- [42] M. Khazaei, M. Arai, T. Sasaki, M. Estili, Y. Sakka, Trends in electronic structures and structural properties of MAX phases: a first-principles study on M₂AlC (M = Sc, Ti, Cr, Zr, Nb, Mo, Hf, or Ta), M₂AlN, and hypothetical M₂AlB phases, *J. Phys. Condens. Matter.* 26 (2014) 505503. <https://doi.org/10.1088/0953-8984/26/50/505503>.
- [43] A. Gencer, G. Surucu, Electronic and lattice dynamical properties of Ti₂SiB MAX phase, *Mater. Res. Express.* 5 (2018) 076303. <https://doi.org/10.1088/2053-1591/aace7f>.
- [44] G. Surucu, Investigation of structural, electronic, anisotropic elastic, and lattice dynamical properties of MAX phases borides: An Ab-initio study on hypothetical MAB (M = Ti, Zr, Hf; A = Al, Ga, In) compounds, *Mater. Chem. Phys.* 203 (2018) 106–117.
<https://doi.org/10.1016/j.matchemphys.2017.09.050>.
- [45] G. Surucu, A. Gencer, X. Wang, O. Surucu, Lattice dynamical and thermo-elastic

- properties of M₂AlB (M = V, Nb, Ta) MAX phase borides, *J. Alloys Compd.* 819 (2020) 153256. <https://doi.org/10.1016/j.jallcom.2019.153256>.
- [46] N. Miao, J. Wang, Y. Gong, J. Wu, H. Niu, S. Wang, K. Li, A.R. Oganov, T. Tada, H. Hosono, Computational Prediction of Boron-Based MAX Phases and MXene Derivatives, *Chem. Mater.* 32 (2020) 6947–6957. <https://doi.org/10.1021/acs.chemmater.0c02139>.
- [47] M.D. Segall, P.J.D. Lindan, M.J. Probert, C.J. Pickard, P.J. Hasnip, S.J. Clark, M.C. Payne, First-principles simulation: ideas, illustrations and the CASTEP code, *J. Phys. Condens. Matter.* 14 (2002) 2717–2744. <https://doi.org/10.1088/0953-8984/14/11/301>.
- [48] S.J. Clark, M.D. Segall, C.J. Pickard, P.J. Hasnip, M.I.J. Probert, K. Refson, M.C. Payne, First principles methods using CASTEP, *Zeitschrift Für Krist. - Cryst. Mater.* 220 (2005). <https://doi.org/10.1524/zkri.220.5.567.65075>.
- [49] J.P. Perdew, K. Burke, M. Ernzerhof, Generalized Gradient Approximation Made Simple, *Phys. Rev. Lett.* 77 (1996) 3865–3868. <https://doi.org/10.1103/PhysRevLett.77.3865>.
- [50] H.J. Monkhorst, J.D. Pack, Special points for Brillouin-zone integrations, *Phys. Rev. B.* 13 (1976) 5188–5192. <https://doi.org/10.1103/PhysRevB.13.5188>.
- [51] T.H. Fischer, J. Almlof, General methods for geometry and wave function optimization, *J. Phys. Chem.* 96 (1992) 9768–9774. <https://doi.org/10.1021/j100203a036>.
- [52] M.A. Ali, A.K.M.A. Islam, Sn_{1-x}BixO₂ and Sn_{1-x}TaxO₂ (0 ≤ x ≤ 0.75): A first-principles study, *Phys. B Condens. Matter.* 407 (2012) 1020–1026. <https://doi.org/10.1016/j.physb.2012.01.002>.
- [53] M.A. Ali, A.K.M.A. Islam, N. Jahan, S. Karimunnesa, First-principles study of SnO under high pressure, *Int. J. Mod. Phys. B.* 30 (2016) 1650228. <https://doi.org/10.1142/S0217979216502283>.
- [54] M.A. Ali, N. Jahan, A.K.M.A. Islam, Sulvanite Compounds Cu₃TMS₄ (TM = V, Nb and Ta): Elastic, Electronic, Optical and Thermal Properties using First-principles Method, *J. Sci. Res.* 6 (2014) 407–419. <https://doi.org/10.3329/jsr.v6i3.19191>.
- [55] F. Mouhat, F.-X. Coudert, Necessary and sufficient elastic stability conditions in various crystal systems, *Phys. Rev. B.* 90 (2014) 224104. <https://doi.org/10.1103/PhysRevB.90.224104>.
- [56] M. Born, On the stability of crystal lattices. I, *Math. Proc. Cambridge Philos. Soc.* 36 (1940) 160–172. <https://doi.org/10.1017/S0305004100017138>.
- [57] R. Hill, The Elastic Behaviour of a Crystalline Aggregate, *Proc. Phys. Soc. Sect. A.* 65 (1952) 349–354. <https://doi.org/10.1088/0370-1298/65/5/307>.
- [58] M.A. Ali, A.K.M.A. Islam, M.S. Ali, Ni-rich Nitrides ANNi₃ (A = Pt, Ag, Pd) in Comparison with Superconducting ZnNNi₃, *J. Sci. Res.* 4 (2011) 1. <https://doi.org/10.3329/jsr.v4i1.9026>.

- [59] W. Voigt, Lehrbuch der Kristallphysik, Vieweg+Teubner Verlag, Wiesbaden, 1966. <https://doi.org/10.1007/978-3-663-15884-4>.
- [60] A. Reuss, Berechnung der Fließgrenze von Mischkristallen auf Grund der Plastizitätsbedingung für Einkristalle., ZAMM - J. Appl. Math. Mech. / Zeitschrift Für Angew. Math. Und Mech. 9 (1929) 49–58. <https://doi.org/10.1002/zamm.19290090104>.
- [61] M.A. Ali, M. Roknuzzaman, M.T. Nasir, A.K.M.A. Islam, S.H. Naqib, Structural, elastic, electronic and optical properties of Cu₃MTe₄ (M = Nb, Ta) sulvanites — An *ab initio* study, Int. J. Mod. Phys. B. 30 (2016) 1650089. <https://doi.org/10.1142/S0217979216500892>.
- [62] M.A. Ali, M. Anwar Hossain, M.A. Rayhan, M.M. Hossain, M.M. Uddin, M. Roknuzzaman, K. Ostrikov, A.K.M.A. Islam, S.H. Naqib, First-principles study of elastic, electronic, optical and thermoelectric properties of newly synthesized K₂Cu₂GeS₄ chalcogenide, J. Alloys Compd. 781 (2018) 37–46. <https://doi.org/10.1016/j.jallcom.2018.12.035>.
- [63] M.M. Hossain, M.A. Ali, M.M. Uddin, M.A. Hossain, M. Rasadujjaman, S.H. Naqib, M. Nagao, S. Watauchi, I. Tanaka, Influence of Se doping on recently synthesized NaInS₂-xSex solid solutions for potential thermo-mechanical applications studied via first-principles method, Mater. Today Commun. 26 (2021) 101988. <https://doi.org/10.1016/j.mtcomm.2020.101988>.
- [64] X.-Q. Chen, H. Niu, D. Li, Y. Li, Modeling hardness of polycrystalline materials and bulk metallic glasses, Intermetallics. 19 (2011) 1275–1281. <https://doi.org/10.1016/j.intermet.2011.03.026>.
- [65] M.A. Ali, M.M. Hossain, N. Jahan, A.K.M.A. Islam, S.H. Naqib, Newly synthesized Zr₂AlC, Zr₂(Al_{0.58}Bi_{0.42})C, Zr₂(Al_{0.2}Sn_{0.8})C, and Zr₂(Al_{0.3}Sb_{0.7})C MAX phases: A DFT based first-principles study, Comput. Mater. Sci. 131 (2017) 139–145. <https://doi.org/10.1016/j.commatsci.2017.01.048>.
- [66] A. Bouhemadou, First-principles study of structural, electronic and elastic properties of Nb₄AlC₃, Brazilian J. Phys. 40 (2010) 52–57. <https://doi.org/10.1590/S0103-97332010000100009>.
- [67] S. Jhi, J. Ihm, S.G. Louie, Electronic mechanism of hardness enhancement in transition-metal carbonitrides, 399 (1999) 1–3.
- [68] H. Gou, L. Hou, J. Zhang, F. Gao, Pressure-induced incompressibility of ReC and effect of metallic bonding on its hardness, Appl. Phys. Lett. 92 (2008) 241901. <https://doi.org/10.1063/1.2938031>.
- [69] M.T. Nasir, M.A. Hadi, M.A. Rayhan, M.A. Ali, M.M. Hossain, M. Roknuzzaman, S.H. Naqib, A.K.M.A. Islam, M.M. Uddin, K. Ostrikov, First-Principles Study of Superconducting ScRhP and ScIrP pnictides, Phys. Status Solidi. 254 (2017) 1700336. <https://doi.org/10.1002/pssb.201700336>.

- [70] M.A. Ali, M.A. Hadi, M.M. Hossain, S.H. Naqib, A.K.M.A. Islam, Theoretical investigation of structural, elastic, and electronic properties of ternary boride MoAlB, *Phys. Status Solidi*. 254 (2017) 1700010. <https://doi.org/10.1002/pssb.201700010>.
- [71] P. Barua, M.M. Hossain, M.A. Ali, M.M. Uddin, S.H. Naqib, A.K.M.A. Islam, Effects of transition metals on physical properties of M₂BC (M = V, Nb, Mo and Ta): A DFT calculation, *J. Alloys Compd.* 770 (2018) 523–534. <https://doi.org/10.1016/j.jallcom.2018.08.155>.
- [72] M.A. Ali, M.M. Hossain, A.K.M.A. Islam, S.H. Naqib, Ternary boride Hf₃PB₄: Insights into the physical properties of the hardest possible boride MAX phase, *J. Alloys Compd.* 857 (2021) 158264. <https://doi.org/10.1016/j.jallcom.2020.158264>.
- [73] S.F. Pugh, XCII. Relations between the elastic moduli and the plastic properties of polycrystalline pure metals, *London, Edinburgh, Dublin Philos. Mag. J. Sci.* 45 (1954) 823–843. <https://doi.org/10.1080/14786440808520496>.
- [74] M. Roknuzzaman, M.A. Hadi, M.A. Ali, M.M. Hossain, N. Jahan, M.M. Uddin, J.A. Alarco, K. Ostrikov, First hafnium-based MAX phase in the 312 family, Hf₃AlC₂: A first-principles study, *J. Alloys Compd.* 727 (2017) 616–626. <https://doi.org/10.1016/j.jallcom.2017.08.151>.
- [75] Y. Zhou, Z. Sun, Electronic structure and bonding properties of layered machinable and ceramics, *Phys. Rev. B - Condens. Matter Mater. Phys.* 61 (2000) 12570–12573. <https://doi.org/10.1103/PhysRevB.61.12570>.
- [76] M.A. Ali, S.H. Naqib, Recently synthesized (Ti_{1-x}Mo_x)₂AlC (0 ≤ x ≤ 0.20) solid solutions: deciphering the structural, electronic, mechanical and thermodynamic properties via ab initio simulations, *RSC Adv.* 10 (2020) 31535–31546. <https://doi.org/10.1039/D0RA06435A>.
- [77] H. Ledbetter, A. Migliori, A general elastic-anisotropy measure, *J. Appl. Phys.* 100 (2006) 063516. <https://doi.org/10.1063/1.2338835>.
- [78] J. Chang, G.-P. Zhao, X.-L. Zhou, K. Liu, L.-Y. Lu, Structure and mechanical properties of tantalum mononitride under high pressure: A first-principles study, *J. Appl. Phys.* 112 (2012) 083519. <https://doi.org/10.1063/1.4759279>.
- [79] H.M. Ledbetter, Elastic properties of zinc: A compilation and a review, *J. Phys. Chem. Ref. Data.* 6 (1977) 1181–1203. <https://doi.org/10.1063/1.555564>.
- [80] A.K.M.A. Islam, A.S. Sikder, F.N. Islam, NbB₂: a density functional study, *Phys. Lett. A.* 350 (2006) 288–292. <https://doi.org/10.1016/j.physleta.2005.09.085>.
- [81] J. Wang, Y. Zhou, T. Liao, Z. Lin, First-principles prediction of low shear-strain resistance of Al₃BC₃: A metal borocarbide containing short linear BC₂ units, *Appl. Phys. Lett.* 89 (2006) 021917. <https://doi.org/10.1063/1.2220549>.
- [82] J.W.C., Anisotropy in single-crystal refractory compounds, *J. Less Common Met.* (1969). [https://doi.org/10.1016/0022-5088\(69\)90173-8](https://doi.org/10.1016/0022-5088(69)90173-8).

- [83] S.I. Ranganathan, M. Ostoja-Starzewski, Universal Elastic Anisotropy Index, *Phys. Rev. Lett.* 101 (2008) 055504. <https://doi.org/10.1103/PhysRevLett.101.055504>.
- [84] R. Gaillac, P. Pullumbi, F.-X. Coudert, ELATE: an open-source online application for analysis and visualization of elastic tensors, *J. Phys. Condens. Matter.* 28 (2016) 275201. <https://doi.org/10.1088/0953-8984/28/27/275201>.
- [85] K. Das, M.A. Ali, M.M. Hossain, S.H. Naqib, A.K.M.A. Islam, M.M. Uddin, Dynamical stability, vibrational, and optical properties of anti-perovskite A_3BX (Ti_3TiN , Ni_3SnN , and Co_3AlC) phases: A first principles study, *AIP Adv.* 10 (2020) 095226. <https://doi.org/10.1063/5.0022376>.
- [86] X. Luo, B. Wang, Structural and elastic properties of $LaAlO_3$ from first-principles calculations, *J. Appl. Phys.* 104 (2008) 073518. <https://doi.org/10.1063/1.2990068>.
- [87] O.L. Anderson, A simplified method for calculating the debye temperature from elastic constants, *J. Phys. Chem. Solids.* 24 (1963) 909–917. [https://doi.org/10.1016/0022-3697\(63\)90067-2](https://doi.org/10.1016/0022-3697(63)90067-2).
- [88] M.A. Ali, M.N.I. Khan, M.M. Hossain, F.-U.-Z. Chowdhury, M.N. Hossain, R. Rashid, M.A. Hakim, S.M. Hoque, M.M. Uddin, Mechanical behavior, enhanced dc resistivity, energy band gap and high temperature magnetic properties of Y-substituted Mg–Zn ferrites, *Mater. Res. Express.* 7 (2020) 036101. <https://doi.org/10.1088/2053-1591/ab7791>.
- [89] G.A. Slack, The Thermal Conductivity of Nonmetallic Crystals, *Solid State Phys. - Adv. Res. Appl.* 34 (1979) 1–71. [https://doi.org/10.1016/S0081-1947\(08\)60359-8](https://doi.org/10.1016/S0081-1947(08)60359-8).
- [90] M.A. Ali, Newly Synthesized Ta based MAX phase $(Ta_{1-x}Hf_x)_4AlC_3$ and $(Ta_{1-x}Hf_x)_4Al_{0.5}Sn_{0.5}C_3$ ($0 \leq x \leq 0.25$) Solid Solutions: Unravelling the Mechanical, Electronic and Thermodynamic Properties, *Phys. Status Solidi.* (2020) pssb.202000307. <https://doi.org/10.1002/pssb.202000307>.
- [91] V.N. Belomestnykh, E.P. Tesleva, Interrelation between anharmonicity and lateral strain in quasi-isotropic polycrystalline solids, *Tech. Phys.* 49 (2004) 1098–1100. <https://doi.org/10.1134/1.1787679>.
- [92] S.I. Mikitishin, Interrelationship of Poisson's ratio with other characteristics of pure metals, *Sov. Mater. Sci.* 18 (1982) 262–265. <https://doi.org/10.1007/BF01150837>.
- [93] R. John, B. Merlin, Optical properties of graphene, silicene, germanene, and stanene from IR to far UV – A first principles study, *J. Phys. Chem. Solids.* 110 (2017) 307–315. <https://doi.org/10.1016/j.jpcs.2017.06.026>.
- [94] M.A. Ali, M.M. Hossain, M.M. Uddin, A.K.M.A. Islam, D. Jana, S.H. Naqib, DFT insights into new B-containing 212 MAX phases: Hf_2AB_2 ($A = In, Sn$), *J. Alloys Compd.* 860 (2021) 158408. <https://doi.org/10.1016/j.jallcom.2020.158408>.
- [95] M.A. Ali, M.S. Ali, M.M. Uddin, Structural, elastic, electronic and optical properties of metastable MAX phase Ti_5SiC_4 compound, *Indian J. Pure Appl. Phys.* 54 (2016) 386–390.

- [96] S. Li, R. Ahuja, M.W. Barsoum, P. Jena, B. Johansson, Optical properties of Ti_3SiC_2 and Ti_4AlN_3 , *Appl. Phys. Lett.* 92 (2008) 221907. <https://doi.org/10.1063/1.2938862>.
- [97] M.M. Hossain, M.A. Hossain, S.A. Moon, M.A. Ali, M.M. Uddin, S.H. Naqib, A.K.M.A. Islam, M. Nagao, S. Watauchi, I. Tanaka, NaInX_2 ($X = \text{S}, \text{Se}$) layered materials for energy harvesting applications: first-principles insights into optoelectronic and thermoelectric properties, *J. Mater. Sci. Mater. Electron.* 0 (2021) 1–14. <https://doi.org/10.1007/s10854-020-05131-7>.